SHEAR CHARACTERISTICS OF WBK AND WBD

Junye Song[1], Gyeong Deuk Ko[2], Ki Won Lee[3] and Ki Ju Kang[2]*

[1]School of Mechanical Systems Engineering, Chonnam National University, Gwang-ju, Korea

[2]Product Performance Evaluation Team, KUMHO TIRE R&D Center, Gwang-ju, Korea

[3]School of Mechanical Systems Engineering, Chonnam National University, Gwang-ju, Korea

* Corresponding author (kjkang@chonnam.ac.kr)

1. Introduction

Wire-woven Bulk KagomUUe (WBK) is a cellular metal invented by Lee and Kang [1], recently. WBK is fabricated by assembling helically-formed wires and brazing cross points among the wires. As the raw materials, metallic wires have intrinsic benefits in aspects of quality control, strengthening and handling. According to their studies [2-4], WBK is better than conventional metal foams in the specific strength, that is, strength per unit weight, and almost equivalent to ideal Kagome truss with straight struts. Moreover, WBK has high potential for mass production.

Last year, Kang and his colleagues [5] introduced a new addition of wire-woven cellular metal fabricated of helically formed wires, i.e., Wire-woven Bulk Diamond (WBD). Fig. 1 shows the configurations of WBD compared with WBK. While Kagome truss which WBK stems from is composed of tetrahedrons and octahedrons, the truss which WBD simulates is composed of regular octahedrons and cub-octahedrons (or vector equilibriums) [6]. Compression tests on WBD revealed that, for a given slenderness ratio, the density and yield strength of WBD were about twice as high as those for WBK, but elastic stiffness of WBD was not that higher than that for WBK. Consequently, WBD would be good for heavy duty applications. In this work, mechanical properties of WBD and WBK under shear loading are studied analytically and numerically compared to each other, and the merit, shortcomings and potential of WBD are discussed.

2 .Analytic Solution

As basic approach, the analytic solutions for stiffness and strength of WBK and WBD under shear loading are derived under assumption that both of them are composed of straight struts and ball-jointed connections rather than the curved ones and brazed joints. Also, it is assumed that the WBK and WBD truss fails only by elastic or plastic buckling of the struts, but never by tensile yielding or brittle fracture. This assumption is reasonable for wires of strain-hardening ductile metal. A slender member like a strut is plastically buckled under compression as soon as the strut starts to yield, if the material has a distinct yield point on its stress-strain curve [7]. The critical forces causing elastic and plastic buckling of a strut, F_{cr}, are given by respectively.

$$F_{cr,elastic} = \frac{\pi^3 E d^4}{64c^2} \tag{1a}$$

$$F_{cr,plastic} = \frac{\pi d^2}{4}\sigma_o \tag{1b}$$

Here, σ_o and E are the yield strength and Young's modulus of the raw material, respectively.

2.1 WBK

Fig. 2 shows configurations of the unit cell of WBK, idealized model, and a tetrahedron from its lower half. Shear failure of WBK is caused by elastic or plastic buckling of one of the three out-of-plane struts in the tetrahedron. Hence, the allowable value of shear force, R_a, applied in the direction ϕ, on the 1-2 plane is the positive minimum of the shear forces which respectively make the longitudinal forces acting in the struts to reach F_{cr} of Eq. (1a) and (1b) as follows;

$$R_a(\phi) = \text{positive minimum of}$$

$$\left(\frac{\sqrt{3}F_{cr}}{2\sin\phi}, \frac{-F_{cr}}{\cos\phi + \frac{\sin\phi}{\sqrt{3}}}, \frac{F_{cr}}{\cos\phi - \frac{\sin\phi}{\sqrt{3}}} \right)$$

Fig. 3 shows the variation of R_a normalized by F_{cr} with ϕ. In this work, two orientations were considered. Orientation-I, ϕ =0, 60°, 120°, 180°, etc., gives R_a=F_{cr} and the same strength in the opposite direction, ϕ +180°. Orientation-II, ϕ =30°, 90°, 150°,

210°, etc., gives $R_a = \sqrt{3}F_{cr}$ or $R_a = \frac{\sqrt{3}}{2}F_{cr}$, that is, different strength in the opposite direction. Dividing R_a by the area, the equivalent shear yield strength of the core, τ_y^c, are derived as follows;

$$\tau_y^c\Big|_{elasticbuckling} = \alpha \frac{\pi^3}{128\sqrt{3}} E\left(\frac{d}{c}\right)^4 \quad (3a)$$

$$\tau_y^c\Big|_{plasticbuckling} = \alpha \frac{\pi}{8\sqrt{3}} \sigma_o\left(\frac{d}{c}\right)^2 \quad (3b)$$

where α is an index indicating the orientation, that is, $\alpha = 1$ for orientation-I and $\alpha = \sqrt{3}/2$ for the lower strength direction in orientation-II.

For WBK idealized with straight struts, the relative density of WBK cores, ρ_{rel}, is expressed by

$$\rho_{rel} = \frac{3\sqrt{2}\pi}{8}\left(\frac{d}{c}\right)^2$$

And applying Castigliano's 2nd theorem, the shear modulus, *G*, is derived as follows;

$$G = \alpha \frac{\sqrt{2}}{24}\pi E\left(\frac{d}{c}\right)^2 \quad (4)$$

where α is an index indicating the orientation, that is, $\alpha = 3/7$ for orientation-I and $\alpha = 9/19$ for orientation-II.

2.2 WBD

Fig. 4 shows configurations of the unit cell of WBD, idealized model, and a pyramid from its lower half. Shear failure of WBD is caused by elastic or plastic buckling of one of the four out-of-plane struts in the pyramid. Hence, the allowable value of shear force, R_a, is given as follows;

$$R_a(\phi) = \text{positive minimum of}$$
$$\left(\frac{2F_{cr}}{\sin\phi + \cos\phi}, \frac{2F_{cr}}{-\sin\phi + \cos\phi}, \frac{-2F_{cr}}{\sin\phi + \cos\phi}, \frac{2F_{cr}}{\sin\phi - \cos\phi}\right)$$

Fig. 5 shows the variation of R_a normalized by F_{cr} with ϕ. In this work, two orientations were considered. Orientation-I, ϕ=0, 90°, gives $R_a = 2F_{cr}$ and the same strength in the opposite direction, ϕ+180°. Orientation-II, ϕ=45°, 135° gives $R_a = \sqrt{2}F_{cr}$, that is, different strength in the opposite direction. Dividing R_a by the area, the equivalent shear yield strength of the core, τ_y^c, are derived as follows;

$$\tau_y^c\Big|_{elastibucling} = \alpha \frac{\pi^3}{128} G\left(\frac{d}{c}\right)^4 \quad (4a)$$

$$\tau_y^c\Big|_{plastibucling} = \alpha \frac{\pi}{8} \sigma_0\left(\frac{d}{c}\right)^2 \quad (4b)$$

where α is an index indicating the orientation, that is, $\alpha = 2$ for orientation-I and $\alpha = \sqrt{2}$ for the lower strength direction in orientation-II.

For WBD idealized with straight struts, the relative density of WBD cores, ρ_{rel}, is expressed by

$$\rho_{rel} = \frac{3\sqrt{2}\pi}{4}\left(\frac{d}{c}\right)^2$$

And applying Castigliano's 2nd theorem, the shear modulus, *G*, is derived as follows;

$$G = \alpha \frac{\sqrt{2}}{16}\pi E\left(\frac{d}{c}\right)^2 \quad (5)$$

where α is an index indicating the orientation, that is, $\alpha = 4/5$ for orientation-I and $\alpha = 2/3$ for orientation-II.

3. Numerical simulation

FE analysis were used to explore the behavior of WBK and WBD cores subjected to shear loading, and were performed using Version 6.5 of the commercially-available ABAQUS code. The cores were modeled with the commercial code PATRAN 2005. Fig. 6 shows the FE model with the applied load and boundary condition. The element type was solid element of 15 nodes (C3D15 in ABAQUS) and the total number of the elements in a model was 157,287 for WBK and 283,152 for WBD.

4. Results and Discussion

Figs. 7(a) and 7(b) show the shear stress-strain curves obtained by Eqs.(3b) and the FEA for WBK with Orientation-I and II, respectively.

Figs. 8(a) and 8(b) show the shear stress-strain curves obtained by Eqs.(4b) and the FEA for WBD with Orientation-I and II, respectively.

The shear strength and stiffness of orientation-I are higher than orientation-II in case of WBK and WBD.

Shear strength is defined as strength level at the strain of 5%. Figs. 9(a) and 9(b) show the strength

normalized by the wire yield strength and relative density for WBK and WBD, respectively.

It showed that the normalized strength of WBK and WBD increase in accordance with the slenderness ratio (*d/c*).

Figs. 10(a) and 10(b) show the stiffness normalized by the wire shear modulus and relative density for WBK and WBD, respectively.

References

[1] K.J. Kang and Y.H. Lee "Three-Dimensional Cellular Light Structures Directly Woven by Continuous Wires and the Manufacturing Method of the Same" Germany Patent Registration No. 11 2004 002 127, 2008.06.27

[2] Y.H. Lee, B.K. Lee, I. Jeon and K.J. Kang "Wire-Woven Bulk Kagome (WBK) truss cores". *Acta Materialia*, Vol. 55, pp 6084-6094, 2007.

[3] B.K. Lee and K.J. Kang "A parametric study on compressive characteristics of Wire-woven bulk Kagome truss cores". *Composite Structures*, Vol. 92, pp 445-453, 2009.

[4] Y.H. Lee, J.E. Choi and K.J. Kang "A Wire-woven Cellular Metal: Part-II, Evaluation by Experiments and Numerical Simulations ". *Materials and Design*, Vol.30, Issue 10, pp.4459-4468, 2009.

[5] G.D. Ko, K.W. Lee and K.J. Kang "Comparative Study of Compressive Characteristics of WBK and WBD", *Cellular Materials*, Proc. of Cellmat2010 edited by G. Stephani, T. Hipke, M. Scheffler and J. Adler, pp.307-312, 2010.

[6] Buckminster Fuller "*Synergetics: Explorations in the Geometry of Thinking*", Macmillan Publishing Co., pp.669, 1975.

[7] Shanely R. "*Mechanics of Materials*", McGraw-Hill, 1967.

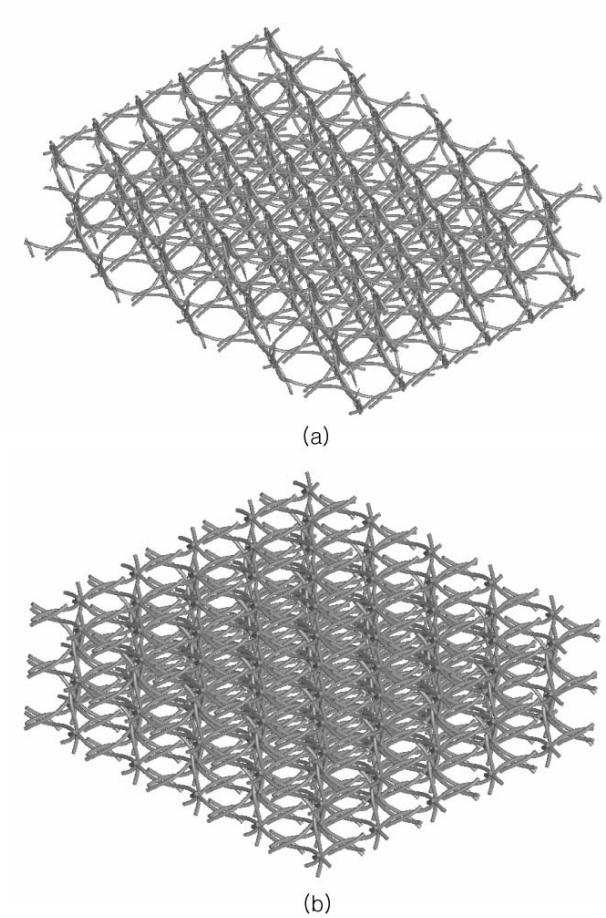

Fig.1. (a) WBK truss and (b) WBD truss.

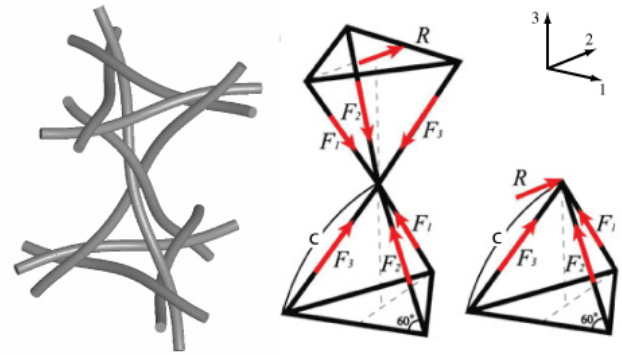

Fig.2. Unit cell of WBK and idealized model under shear loading

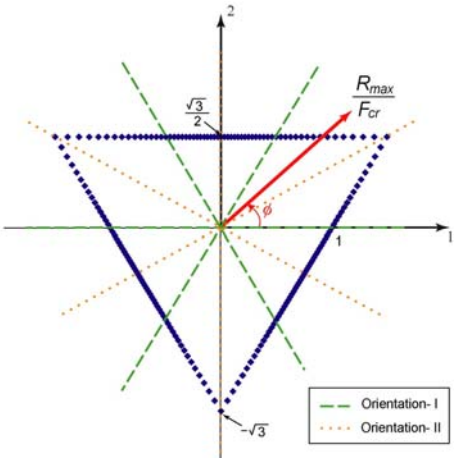

Fig.3. Orientation of WBK under shear loading

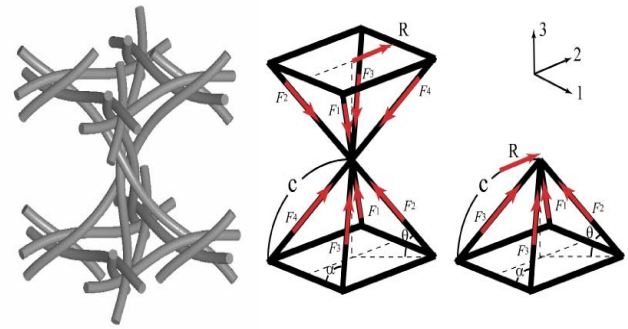

Fig.4. Unit cell of WBD and idealized model under shear loading

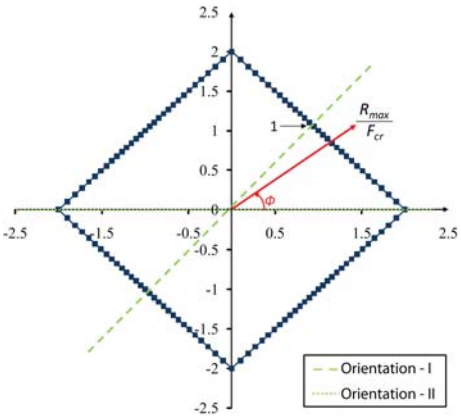

Fig.5. Orientation of WBD under shear loading

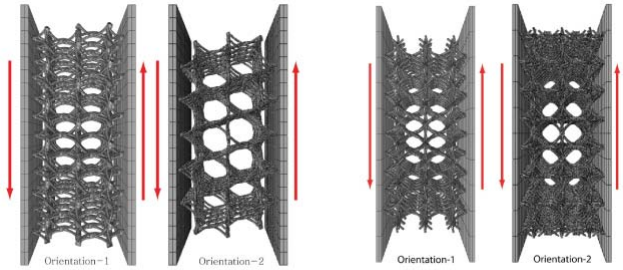

(a) WBK (b) WBD

Fig.6. The finite-element model of WBK and WBD sandwiches with applied shear loads by orientation-I and orientation-II.

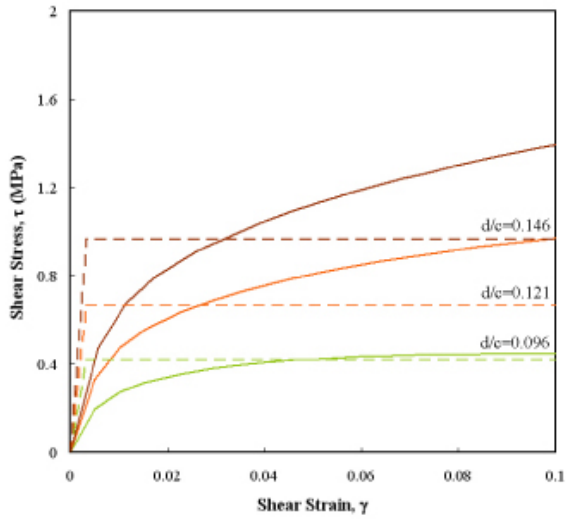

(a) Orientation - I

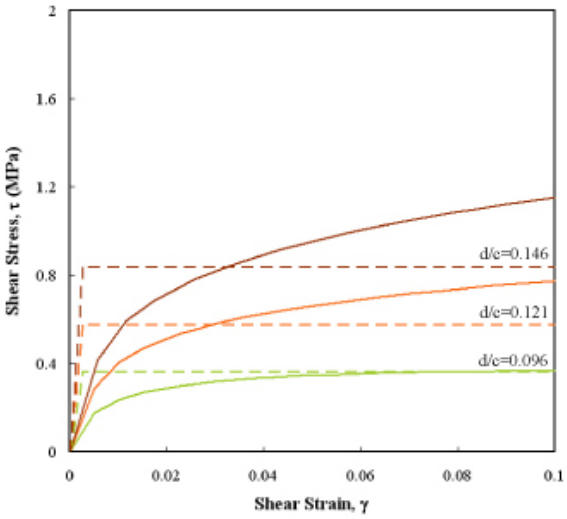

(b) Orientation - II

Fig.7. Stress – strain curves of WBK under shear loading by orientation I and II

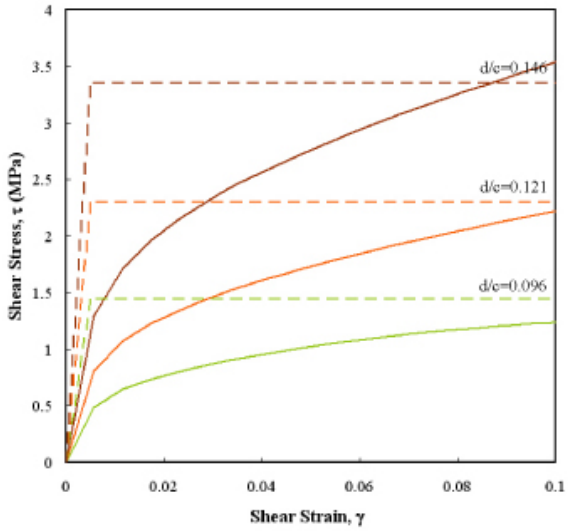

(a) Orientation - I

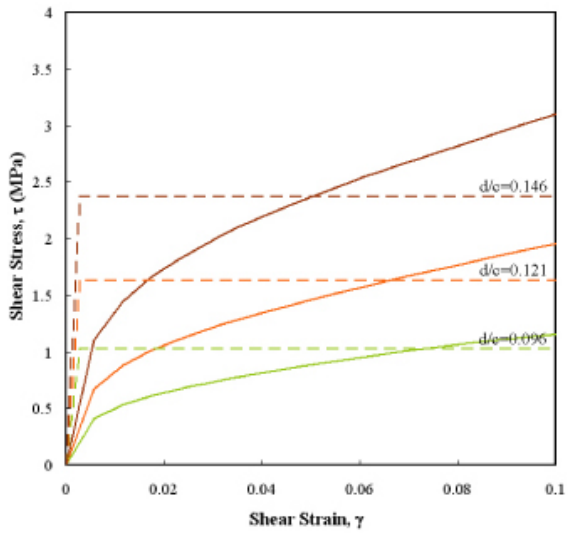

(b) Orientation - II

Fig.8. Stress – strain curves of WBD under shear loading by orientation I and II

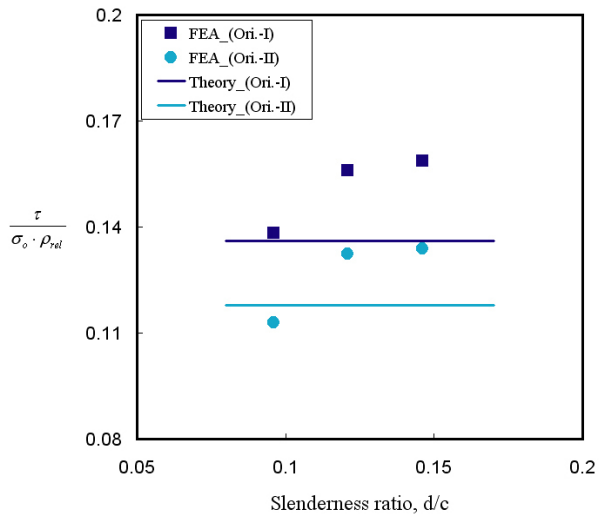

(a) WBK

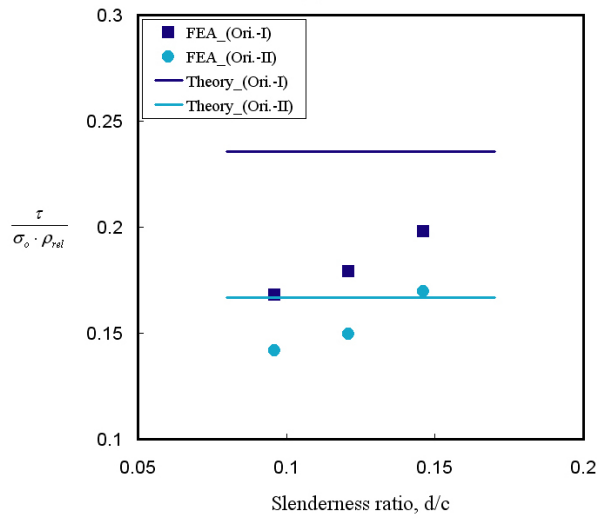

(b) WBD

Fig.9. Normalized strength versus slenderness ratios

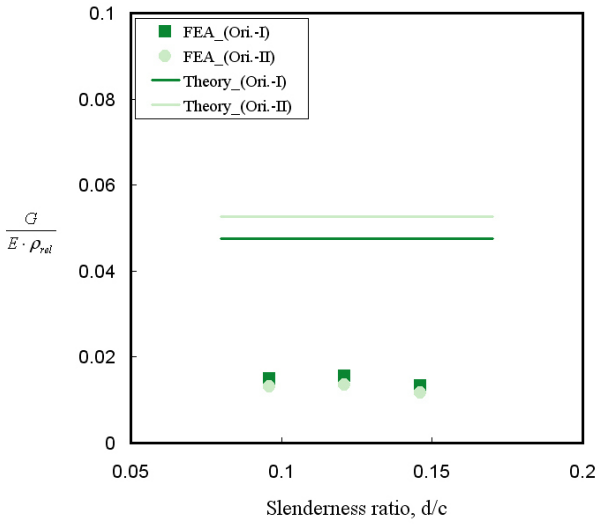

(a) WBK

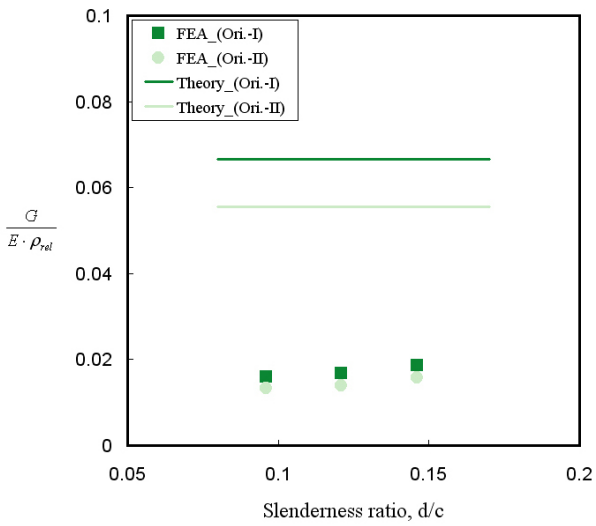

(b) WBD

Fig.10. Normalized stiffness versus slenderness ratios